

Synergism of C₅N Six-Membered Ring and Vapor–Liquid–Solid Growth of CN_x Nanotubes with Pyridine Precursor

Hong Chen, Yong Yang, Zheng Hu,* Kaifu Huo, Yanwen Ma, and Yi Chen

Key Laboratory of Mesoscopic Chemistry of MOE and Jiangsu Provincial Lab for NanoTechnology, School of Chemistry and Chemical Engineering, Nanjing University, Nanjing 210093, China

Xiaoshu Wang

Center for Materials Analysis, Nanjing University, Nanjing 210093, China

Yinong Lu

College of Materials Science and Engineering, Nanjing University of Technology, Nanjing 210093, China

Received: April 10, 2006; In Final Form: June 30, 2006

A series of bamboo-like CN_x nanotubes have been synthesized from pyridine precursor by chemical vapor deposition with bimetallic Fe–Co/ γ -Al₂O₃ catalyst in the range of 550–950 °C. An unusual predominance of pyridinic nitrogen over graphitic nitrogen has been observed for the CN_x nanotubes with reaction temperature below 750 °C. The pyridinic nitrogen decreases and the graphitic nitrogen increases with rising reaction temperature. A synergism mechanism of C₅N-six-membered-ring-based growth through surface diffusion and vapor–liquid–solid growth through bulk diffusion was accordingly deduced and schematically presented. This mechanism could not only explain our own experimental results, but also understand the CN_x-nanotube-related experimental phenomena in the literature, as well as be in accordance with the basic principle of diffusion kinetics. A promising route to the challenging topic for synthesizing regularly arranged C₅N or high-N-content CN_x nanotubes has also been suggested.

Introduction

In the past decades, carbon nanotubes (CNTs) have attracted great research interests due to their novel structures, superior properties, and wide potential applications.¹ Many properties of CNTs are highly dependent on their chirality, diameters, and structural defects which are usually difficult to control experimentally. Doping with different elements is a promising method to tailor the electronic properties of CNTs.² Doping with nitrogen is particularly interesting since the electronic properties of the CN_x nanotubes thus obtained are primarily determined by their compositions.³ Hence, great efforts have been devoted to the preparation of CN_x nanotubes, and many methods such as magnetron sputtering,⁴ arc discharge,^{2a} and chemical vapor deposition (CVD)^{3b–e,5,6,7} have been employed for this purpose. CVD method is regarded as the most promising approach for its mild condition, low cost, and possible large-scale production. Different kinds of precursors, including C- and N-containing molecules such as C₅H₅N,⁶ CH₃CN,^{3d} and HOCN(CH₃)₂,^{5f} or mixtures of C-containing/N-containing gaseous species such as CH₄/N₂^{7a,b,d} and C₂H₂/NH₃^{7c,e,f} have been used for the synthesis of CN_x nanotubes. In most cases, the growth temperature of CN_x nanotubes is in the range of 700–1100 °C, and the average nitrogen content is around 2–10 at. %.^{5,6} It is seen that CN_x nanotubes usually have a defective bamboo-like structure with distinctive compartment layers due to the doping of nitrogen and the nitrogen atoms are bonded to carbon in two forms of pyridinic nitrogen and graphitic nitrogen.^{3b–d,5a,c,d,6,7d–f,8} The

vapor–liquid–solid (VLS) growth mechanism, which is commonly regarded as the supersaturated precipitation of the bulk-diffused species within liquid catalyst, is usually employed to understand the chemistry involved.^{6c,7d,e,9} Very recently, in our CVD synthesis of CNTs with benzene precursor it is found that, with suitable catalyst at relatively low temperature around 645 °C, the C–H bonds of benzene precursor could be selectively dissociated while the C–C connections were retained.^{10a} Accordingly, CNTs could be built up through surface diffusion with the dehydrogenated benzene rings as the building units, and well-graphitized and highly productive quasi-aligned CNTs have been produced.¹⁰ This six-membered-ring-based (C₆-based) growth mechanism has been confirmed by using the in situ thermal analysis–mass spectroscopic (TA-MS) technique, combined with transmission electron microscopic characterization of the CNT product.^{10a} It is noted that the C- and N-containing pyridine molecule possesses a C₅N six-membered ring, similar to a benzene ring. Thus, it is worth exploring the selective dissociation of the C–H bonds of pyridine for the possible construction of C₅N nanotubes with the building units of C₅N six-membered rings. Although pyridine has ever been used for CVD synthesis of CN_x nanotubes in the literature,⁶ the reaction temperature seems to be considerably high, usually >700 °C, hence the C₅N six-membered rings should already be broken.¹¹ According to the above analysis, in this paper, the dehydrogenated bimetallic catalyst of Fe–Co/ γ -Al₂O₃, which is very effective in our CNTs synthesis from benzene,¹⁰ has been applied to the catalytic synthesis of CN_x nanotubes from pyridine at low temperature beneficial for retaining its ring structure. It is found that nitrogen atoms mainly

* To whom correspondence should be addressed. E-mail: zhenghu@nju.edu.cn. Tel.: 0086-25-83686015. Fax: 0086-25-83686251.

exist as pyridinic nitrogen rather than graphitic nitrogen in the obtained CN_x nanotubes, which is contrary to the cases in the literature^{3b-d,5a,c,d,6a-d,7d-f,8} but is consistent with what we expected. In addition, with reaction temperature rising in the range of 550~950 °C, the relative ratio of pyridinic nitrogen in CN_x nanotubes gradually decreases and that of graphitic nitrogen increases, and the N content shows a decreasing tendency, indicating the increasing broken pyridine rings. These results indicate that the C₅N six-membered rings partly played as the building units for constructing the CN_x nanotubes, especially in the low-temperature region. A synergism mechanism of competitive C₅N-six-membered-ring-based growth through surface diffusion with vapor–liquid–solid growth through bulk diffusion was deduced accordingly. It is also suggested that further exploration for a more highly selective dehydrogenated catalyst for pyridine is a valuable and challenging topic for synthesizing regularly arranged C₅N or high-N-content CN_x nanotubes.

Experimental Section

The dehydrogenated bimetallic catalyst of Fe–Co/ γ -Al₂O₃ (1.01 mmol/g Fe–2.01 mmol/g Co/ γ -Al₂O₃), the experimental apparatus, and procedure used in this study are similar to those reported in our previous studies on CNTs.^{10b,c} The catalyst was obtained by 5 h calcination of corresponding γ -Al₂O₃-supported nitrides at 450 °C in air, hence originally the Fe and Co components were in oxide state. Then, about 20 mg catalyst powder was placed in the central part of a horizontal quartz tube in the furnace. After the reaction chamber was evacuated and flushed with N₂ for several times to remove oxygen and moisture, the reactor was heated to the reaction temperature, e.g. 650 °C at a rate of 10 °C/min in N₂. Pyridine was then switched into the system for about 60 min, by the carrying gas of N₂ at a flow rate of 60 mL/min passing through a pyridine saturator at room temperature. The feed rate of pyridine was estimated to be about 10 mg/min. After that, the reactor was cooled in N₂ and a dark spongelike product was obtained. For comparison, CNTs were also synthesized at 650 °C from benzene precursor with the same other conditions. The as-prepared products were characterized by transmission electron microscopy (TEM, JEOL-JEM-1005) and high-resolution TEM (HRTEM, JEM2010). The N/C atomic ratio was analyzed by X-ray photoelectron spectroscopy (XPS, VG ESCALAB MK-II) excited by an X-ray source of Mg K α ($h\nu$ = 1253.6 eV) in an ultrahigh vacuum chamber with a base pressure of $<2 \times 10^{-8}$ Torr. A Raman spectrometer (J Y HR800) was used to evaluate the influence of N-doping on the overall crystallinity of the CN_x nanotubes.

Results and Discussion

Figure 1 shows the TEM images of the nanotubular products, known as the CN_x nanotubes by late characterization, which were synthesized in the temperature range of 550~950 °C. As seen, the nanotubes exhibit the characteristic bamboo-like defective appearance of CN_x nanotubes, which is further revealed by the typical HRTEM images as shown in Figure 2a–e. The typical EDX spectrum in Figure 2f confirms the existence of nitrogen in the nanotubes. The average diameter of the CN_x nanotubes demonstrates an increasing tendency with temperature, which should result from the aggregation of catalyst particles. The conical catalysts were observed to affix to the tips of CN_x nanotubes, similar to the cases for CVD-grown CN_x nanotubes in the literature.^{7d,e} From Figure 2a–e, it is also learned that, as the reaction temperature is increased, the

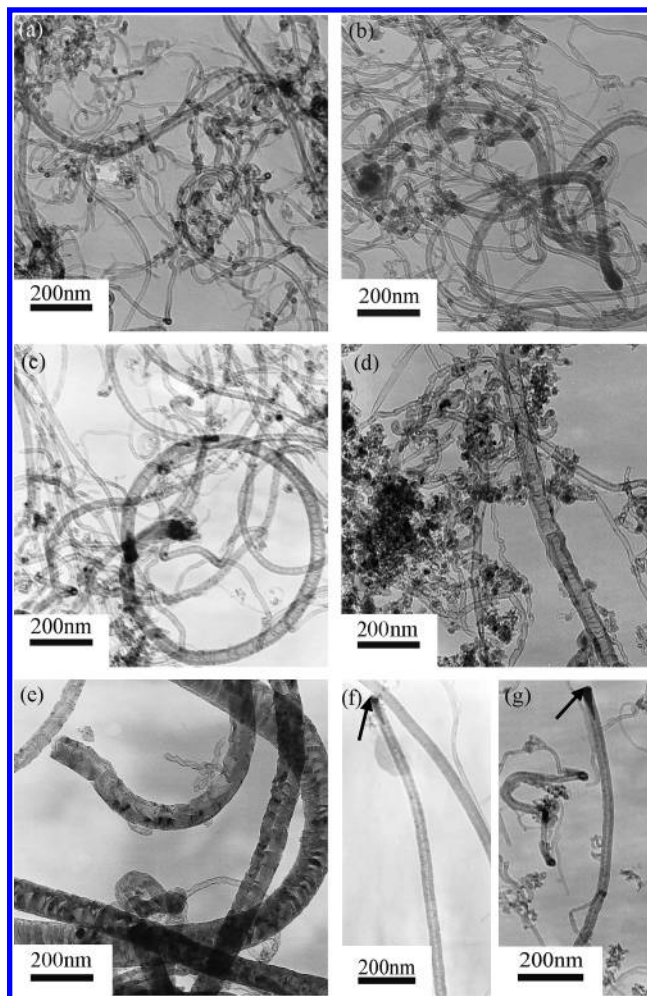


Figure 1. Typical TEM images of CN_x nanotubes synthesized at (a) 550 °C, (b) 650 °C, (c) 750 °C, (d) 850 °C, and (e) 950 °C. Parts f and g show the typical root morphology of the CN_x nanotubes from samples b and c, respectively. The arrows point to the conical catalysts affixed to the tips of the nanotubes.

domains become straighter and less corrugated, which correlates with the synergism growth mechanism of the products as discussed later.

Figure 3a displays the N1s XPS spectra of the CN_x nanotubes synthesized at different temperatures. Each spectrum is mainly composed of two peaks, P1 and P2, around 399.1 and 401.3 eV, respectively, through Gaussian fitting. P1 comes from the pyridine-like N atoms, i.e., the nitrogen in a ring structure folding only two carbon atoms, called pyridinic nitrogen, and P2 from the graphite-like structures, i.e., the sp² nitrogen in the hexagonal rings of a graphite structure, called graphitic nitrogen.^{3b-d,5a,c,d,6,7d-f,8,12}

The total nitrogen content in the CN_x nanotubes obtained from XPS detection, as well as the pyridinic and graphitic nitrogen contents derived from their relative peak intensity, depends on the reaction temperature (T_R) as plotted in Figure 3b. It is seen that, in the low-temperature side with T_R below 750 °C, more than half of the nitrogen exists as pyridinic nitrogen and even about 76% nitrogen as pyridinic nitrogen for the sample with T_R = 550 °C. With increasing T_R , the pyridinic nitrogen decreases obviously (●, Figure 3b) while the graphitic nitrogen increases (▲, Figure 3b) gradually, resulting in the decreasing intensity ratio of P1 to P2, i.e., I_{P1}/I_{P2} , as reflected in the profiles' change in Figure 3a and I_{P1}/I_{P2} vs T_R curve in Figure 3b (□). The total nitrogen content decreases from the highest value of

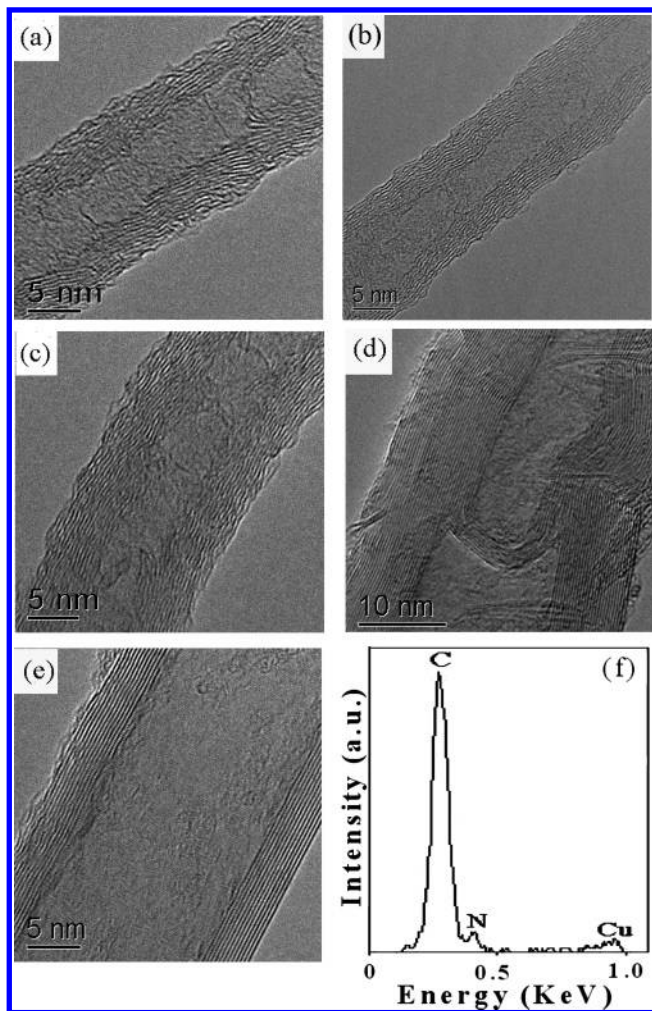


Figure 2. Typical HRTEM images of the CN_x nanotubes synthesized at (a) 550 °C, (b) 650 °C, (c) 750 °C, (d) 850 °C, and (e) 950 °C, respectively. (f) Typical EDX spectrum of the samples. Specifically this one comes from sample b.

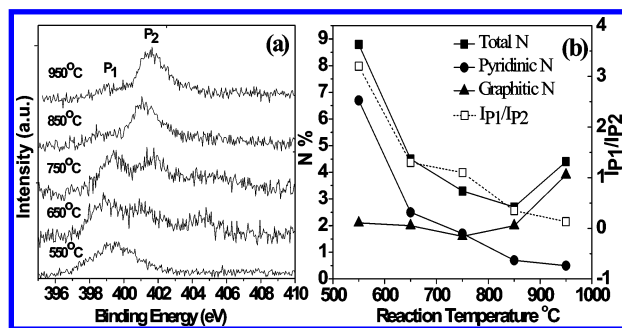


Figure 3. (a) N1s XPS spectra of the CN_x nanotubes synthesized in the temperature range of 550~950 °C. (b) The contents of the total N (■), derived pyridinic N (●), and derived graphitic N (▲) in the samples (refer to left Y axis) together with the profile of I_{P1}/I_{P2} (□) vs reaction temperature (refer to right Y axis). I_{P1} and I_{P2} denote the peak intensity of pyridinic N and graphitic N, respectively.

8.8% for $T_R = 550$ °C to the lowest one of 2.7% for $T_R = 850$ °C, then a little increase to 4.4% for $T_R = 950$ °C, as plotted in Figure 3b (■). As known, both pyridinic nitrogen and graphitic nitrogen will induce an increase in the D band in the Raman spectrum of the N-doped CNTs^{2b,3c,3e,7c} because the hexagonal symmetry of graphite is broken. Hence the intensity ratio of the D mode to G mode (I_D/I_G) in the Raman spectrum should

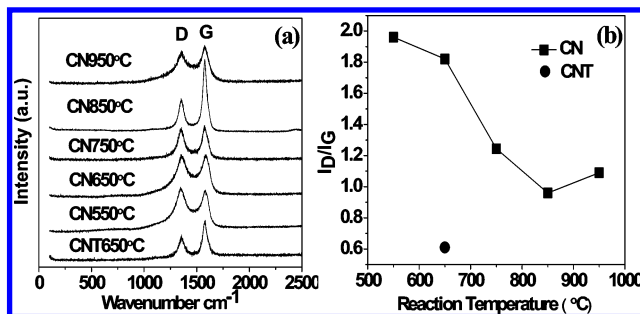


Figure 4. (a) Raman spectra of the CN_x nanotubes synthesized in the temperature range of 550~950 °C. (b) The intensity ratio of D mode to G mode (I_D/I_G) changes with reaction temperature. Raman spectrum and I_D/I_G for CNTs synthesized at 650 °C from benzene precursor are also presented for comparison.

approximately correspond to the total nitrogen content. The Raman spectra and the derived profile of I_D/I_G vs T_R for these samples are shown in Figure 4. It is seen that, as expected, the profile of I_D/I_G vs T_R (Figure 4b) has the similar changing trend to the profile of the total nitrogen content vs T_R (■, Figure 3b), and the I_D/I_G value for the sample of 850 °C with the lowest N content is most close to that for CNTs there for comparison.

It is really unusual and interesting that, in our CN_x nanotubes with T_R below 750 °C, pyridinic nitrogen takes a dominant position over graphitic nitrogen. This was rarely observed in previous XPS and EELS studies in the literature.^{3b-d,5a,c,d,6a-d,7d-f,8} As known, the annealing experimental studies on both CN_x nanotubes and films have indicated that the graphite-like nitrogen is more stable than the pyridine-like nitrogen.^{5d,8} Hence nitrogen atoms would like to conform to the graphite-like configuration for higher stability. Actually this is also evidenced by the numerous experimental results of the predomination of graphitic nitrogen over pyridinic nitrogen for the CN_x nanotubes in the literature,^{3b-d,5a,c,d,6a-d,7d-f,8} even for the CN_x nanotubes synthesized at the temperature as low as 550 °C with N₂ and CH₄ feedstock.^{7d} Therefore, the unusual predomination of pyridinic nitrogen over graphitic nitrogen in this work should imply a new mechanism for the growth of CN_x nanotubes. Enlightened by the C₆-based growth mechanism of CNTs from benzene, a competitive C₅N-six-membered-ring-based (C₅N-based) growth through surface diffusion could be deduced for the catalytic synthesis of CN_x nanotubes from pyridine according to the above experimental results.

As marked by the arrows in Figure 1f and 1g, the conical catalysts are observed to affix to the tips of the CN_x nanotubes. This seems to be the indicative of VLS growth, similar to the cases for the syntheses of CN_x nanotubes in the literature.^{7d,e} However, this is not the complete story of the growth mechanism here. A synergism of the VLS growth through bulk diffusion and a competitive C₅N-based growth through surface diffusion functions during the synthesis of our CN_x nanotubes. In other words, both bulk diffusion and surface diffusion growth contribute to the formation of CN_x nanotubes simultaneously or alternatively. The actual contributions from the two cases which are schematically shown in panels A and B of Figure 5, respectively, depend on the reaction conditions such as the reaction temperature, the sizes of the diffusion species as well as the catalyst properties.

At low T_R of 550 °C, considerable pyridine molecules were selectively dehydrogenated on the catalyst surface, and the C₅N rings thus produced incorporated into the growing CN_x nanotubes through surface diffusion (Figure 5A). Consequently, the

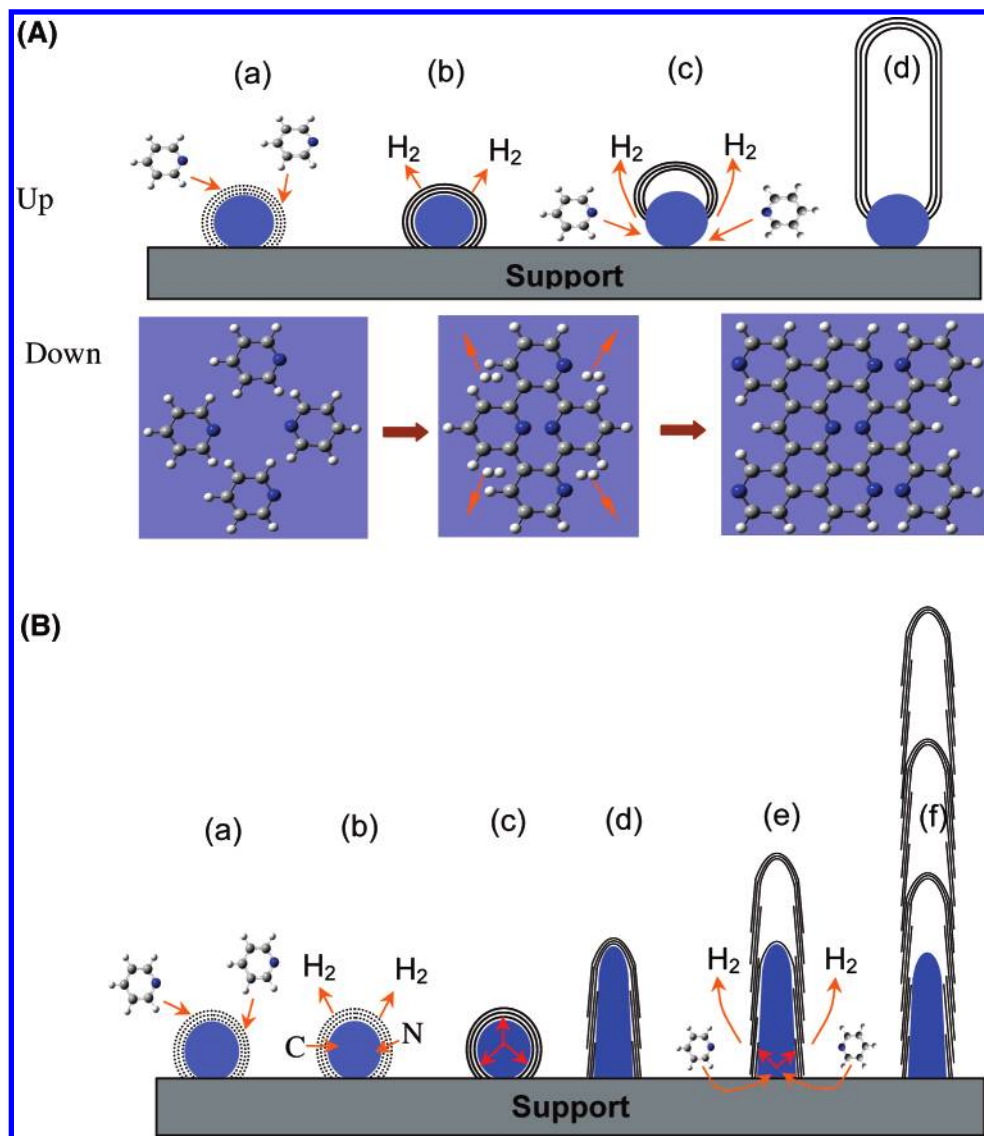


Figure 5. (A) **Up:** Schematic illustration of the C₅N-six-membered-ring-based growth of C₅N nanotubes with pyridine precursor: (a) absorption of pyridine molecules on catalyst surface; (b) dehydrogenation of the pyridine molecules and subsequent assembly of C₅N rings to form graphene-like sheets through surface diffusion; (c) strain-induced formation of nanotubular seed and sequential incorporation of C₅N rings into the interface junction for continuous growth of C₅N nanotube; (d) final state of C₅N nanotube with pyridinic nitrogen. **Down:** The speculative construction of C₅N graphite-like sheet from C₅N six-membered rings, corresponding to b–d in the up illustration. Gray dot, C; Blue dot, N; white dot, H. (B) Schematic illustration of the VLS growth for bamboo-like CN_x nanotubes with pyridine precursor: (a) absorption of pyridine molecules on catalyst surface; (b) dehydrogenation and cracking of the C₅N rings, and subsequent diffusion of the C and N species into bulk catalyst; (c) supersaturation and precipitation of graphene-like CN_x sheets; (d) stretching the catalyst particle into conical shape;^{7d} (e) the truncated CN_x cone was pushed up by the increasing strain due to the growth of the interface CN_x sheets on the side surface and the recovering tendency of the catalyst to its original shape;^{7d} (f) forming a CN_x nanotube by repeating d and e.

CN_x nanotubes were doped with a high nitrogen content of 8.8%, wherein the pyridinic nitrogen dominates over graphitic nitrogen. Meanwhile, the small fragments such as C and N species from the broken pyridine should also enter into the growing CN_x nanotubes through surface diffusion since the catalyst is crystalline^{13c} and the bulk diffusion is negligible^{13b} at such low temperature. With increasing T_R , the selective dehydrogenation was gradually reduced and the number of broken C₅N rings of pyridine molecules increased simultaneously. The C and N species increasingly diffused into the quasi-liquid catalyst to contribute to the growth of CN_x nanotubes in VLS manner (Figure 5B), and the N atoms prefer occupying the positions as graphitic nitrogen rather than pyridinic nitrogen for higher stability.^{5d,8} As a result, the content of pyridinic nitrogen and the relative intensity of P1 for pyridinic nitrogen to P2 for graphitic nitrogen decreased gradually (Figure 3). Similar

experimental law could also be inferred from the data about the synthesis of nitrogen-alloyed activated carbon fibers via pyridine.^{6a} When T_R is higher than 820 °C, almost all the pyridine molecules are broken.¹¹ Hence in this high-temperature side, VLS mechanism dominates the growth of the N-doped CNTs which could result in the slight increase of N content with temperature. A similar phenomenon was also observed in the literature;^{7c} probably it is easier for N atoms to incorporate into the graphite-like structures in higher temperature. Therefore, in the whole temperature range, the pyridinic nitrogen decreases with increasing T_R (●, Figure 3b) since pyridinic nitrogen mainly comes from surface diffusion of the unbroken C₅N units, while the graphitic nitrogen keeps approximately unchanged below 850 °C and then slightly increases (▲, Figure 3b) since graphitic nitrogen mainly comes from VLS growth of the N atoms from the broken C₅N units. The synergism of these two factors results

in the decrease of the total nitrogen content in the range of 550–850 °C, then a slight increase to 950 °C, as plotted in Figure 3b (■). It is known that pyridine-like N sites take the ‘cavities’ or ‘edges’ configuration which should be responsible for the roughness and corrugation in the N-doped carbon nanotubes.^{3c} This is in agreement with the evolution of HRTEM images that the domains become straighter and less corrugated with increasing T_R , i.e., with decreasing pyridine-like N content, as shown in Figure 2a–e. As discussed above, the relative contribution from the VLS growth (Figure 5B) to that from the C₅N-six-membered-ring-based growth (Figure 5A) increases with increasing T_R . Accordingly, the bamboo-like structure becomes dominant with increasing T_R as reflected in Figure 1.

This synergism mechanism could also be taken to understand the experimental results about CN_x nanotubes in the literature. For example, it was generally reported that graphitic nitrogen dominates the nitrogen configuration over pyridinic nitrogen even with pyridine precursor.^{3b–d,5a,c,d,6a–d,7d–f,8} This resulted from the too high reaction temperature (usually 850–1100 °C), at which pyridine molecules could be cracked as reflected in previous literatures.¹¹ Hence, the competitive C₅N-based growth (Figure 5A) through surface diffusion was largely suppressed, and the VLS mechanism (Figure 5B) dominated the growth of CN_x nanotubes. Consequently, the nitrogen atoms prefer conforming to the graphite-like configuration for higher stability.^{5d,8} As for the increase of the pyridinic N in CN_x nanotubes by adding NH₃ to pyridine precursor,^{6e} it is also understandable with this synergism mechanism. Since NH₃ itself could be a product of pyridine pyrolysis, the addition of NH₃ to the system could prevent the pyridine pyrolysis, and much more N will enter into CN_x nanotubes in the form of C₅N ring, which resulted in the increase of pyridine-like N as well as the total N content. As for the cases with separate C-containing and N-containing precursors, such as CH₄/N₂^{7a,b,d} and C₂H₂/NH₃,^{7c,e,f} no C₅N rings pre-existed or few C₅N rings could be preformed during synthesis even at the temperature as low as 550 °C.^{7d} Therefore, the nitrogen atoms still prefer to occupy the positions as graphitic nitrogen rather than pyridinic nitrogen through diffusion.

It seems that the synergism mechanism is also intuitively acceptable. As known, in the commonly accepted VLS model, the catalyst forms a liquid droplet at an elevated temperature and preferentially adsorbs the growth species from the surrounding vapor. The solid whisker-like product grows from this supersaturated eutectic liquid in such a manner making the liquid–solid interface energy the least. For instance, the growth of carbon nanotubes (CNTs) or carbon nanofibers (CNFs)^{9e,f} usually contains four fundamental steps: (1) adsorption of gaseous precursor on catalyst surface, (2) dissociation of the precursor molecules, (3) diffusion of the carbon atoms into the catalyst particle, (4) supersaturation, nucleation, and growth of CNTs or CNFs. Usually surface diffusion is neglected in the classical VLS model. However, it seems that surface diffusion of carbon atoms should exist in step 3, i.e., after the dissociation of the precursor molecules on catalyst surface. Actually recent progress indicates that surface diffusion does exist and could contribute to the formation of CNTs.^{10a,13} Therefore, it is reasonable to speculate that surface diffusion and bulk diffusion should generally coexist. The problem is that it is difficult to distinguish their contribution to the product by routine characterization, which might be the reason for the longtime neglect of the important surface diffusion. By taking surface diffusion into consideration, the growth mechanism might be revealed more correctly, completely, and deeply. This is of course scientifically interesting and technologically important.

The contributions of these two diffusions to the final product should mainly depend on the reaction temperature and the diffusing species itself. Hofmann et al. have summarized the temperature dependence of carbon diffusion in nickel^{13b} from the data by Diamond et al.^{14a} and Mojica et al.^{14b} It is indicated that low temperature is in favor of the surface diffusion while high temperature the bulk diffusion. Anyhow, these two diffusions coexist. In addition, the size of the diffusing species is also a crucial factor to determine its diffusion. An experiential formula about the bulk diffusion¹⁵ indicates that the bulk diffusion coefficient, expressed as $D = k_B T / 4\pi\mu R_0$, is in inverse proportion to the size, R_0 , of the solute. So it is harder for large-size species to diffuse into the liquid catalyst. By applying the above analysis to our case, for the dehydrogenated pyridine, i.e. the C₅N ring, its dissolving into the catalyst is difficult since its size is very large. Actually, since the atomic arrangement of the metallic catalyst is closely packed and the distance between two adjacent atoms is at the atomic level, the large-sized C₅N ring containing six atoms is too difficult to diffuse into the voids between the metal atoms especially at low-temperature side. Therefore, the C₅N rings could only incorporate into the growing CN_x nanotubes through surface diffusion. Obviously, the nitrogen atoms doped into the graphitic-like sheets of the CN_x nanotubes through such manner exist as pyridinic nitrogen. As for the C and N atoms from the cracked pyridine, they could diffuse both in and on the catalyst particle due to their small sizes. Bulk diffusion might dominate over surface diffusion at high-temperature side while quite the reverse at low-temperature side.^{13b} However, their contributions to the product are undistinguishable. Anyhow, the nitrogen atoms incorporated into the graphitic-like sheets mainly as graphitic nitrogen for higher stability.^{5d,8}

According to the above results and analysis, we have learned that both bulk diffusion and surface diffusion could contribute to the growth of CN_x nanotubes. Their relative contribution depends on the experimental conditions such as reaction temperature and the size of the species. Low temperature and large size is helpful for surface diffusion growth while high temperature and small size are in favor of bulk diffusion. In the case of very low temperature, e.g. 550 °C, the catalyst is crystalline,^{13c} and only the surface diffusion of C₅N rings and small fragments from broken pyridine are responsible for the growth of CN_x nanotubes, while the bulk diffusion could be negligible. Hence, this synergism mechanism of C₅N ring and VLS for the growth of CN_x nanotubes could not only explain our own experimental results, but also understand the related experimental phenomena in the literature, as well as be in accordance with the basic principle of diffusion kinetics. Actually, surface diffusion and bulk diffusion should generally coexist in the VLS-type growth of one-dimensional nanostructures, although the surface diffusion has been neglected for a long time^{9e} until very recently.^{10a,13} Anyhow, their synergism has never been dealt with so far probably due to the difficulty in distinguishing their contributions to the products. In our case, the surface diffusion species of C₅N rings are totally different from the bulk diffusion one, and the corresponding N atoms in product occupy different positions and are distinguishable; therefore the synergism mechanism could be experimentally revealed, which is different from the cases in the literature. We believe that the synergism mechanism on the growth of CN_x nanotubes in this work could be valuable for activating further study on the significant topic of the growth mechanism for the important one-dimensional nanostructures as well as guiding our coming research. For example, by optimizing highly

selective dehydrogenated catalyst for pyridine, the C₅N six-membered rings could be largely generated to assemble regularly arranged C₅N nanotubes with all the pyridine-like N and definite chirality of great importance, as Figure 5A suggested. By balancing the weight of the C₅N-ring and VLS models, the nitrogen content of CN_x nanotubes and the properties thereof could be regulated in a wide range. These are challenging topics ahead.

Conclusion

In conclusion, a series of bamboo-like CN_x nanotubes have been catalytically synthesized from pyridine in the range of 550–950 °C and well characterized by different experimental methods. An unusual predominance of pyridinic nitrogen over graphitic nitrogen has been observed for the CN_x nanotubes with *T_R* below 750 °C. The pyridinic nitrogen decreases and the graphitic nitrogen increases with rising *T_R*, resulting in the decreasing of the total nitrogen content in 550–850 °C and then a slight increasing to 950 °C. On the basis of these experimental results, a synergism mechanism of competitive C₅N-six-membered-ring-based growth through surface diffusion with vapor–liquid–solid growth through bulk diffusion was proposed. This mechanism could also explain the experimental phenomena about the growth of CN_x nanotubes in the literature and is consistent with the basic principle of diffusion kinetics. Accordingly, the challenging topic for the synthesis of regularly arranged C₅N or high-N-content CN_x nanotubes could be promising by optimizing the more highly selective dehydrogenated catalyst for pyridine. This deserves our further efforts.

Acknowledgment. This work was financially supported by NSFC (20525312, 20471028), “863” Project (2003AA302150), High-Tech Project of Jiangsu Province (BG2003029), Chinese Ministry of Education (20040284006, NCET-04-0449, 02110), as well as China Postdoctoral Science Foundation (2004035210).

Supporting Information Available: Gaussian fitting results of the N1s XPS spectra, a discussion on the importance of CN_x nanotubes with dominative pyridine-like nitrogen, a discussion on the weak peak around 405 eV in XPS data, and a brief explanation on the paper title. This material is available free of charge via the Internet at <http://pubs.acs.org>.

References and Notes

- (1) (a) Iijima, S. *Nature* **1991**, *354*, 56. (b) *Carbon Nanotubes*; Dresselhaus, M. S.; Dresselhaus, G.; Avouris, Ph., Eds.; Springer: Berlin, 2001. (c) Poncharal, P.; Wang, Z. L.; Ugarte, D.; de Heer, W. A. *Science* **1999**, *283*, 1513. (d) Zhang, M.; Fang, S. L.; Zakhidov, A. A.; Lee, S. B.; Aliev, A. E.; Williams, C. D.; Atkinson, K. R.; Baughman, R. H. *Science* **2005**, *309*, 1215.
- (2) (a) Stephan, O.; Ajayan, P. M.; Colliex, C.; Redlich, Ph.; Lambert, J. M.; Bernier, P.; Lefin, P. *Science* **1994**, *266*, 1683. (b) Chan, L. H.; Hong, K. H.; Xiao, D. Q.; Hsieh, W. J.; Lai, S. H.; Shih, H. C.; Lin, T. C.; Shieu, F. S.; Chen, K. J.; Cheng, H. C. *Appl. Phys. Lett.* **2003**, *82*, 4334.
- (3) (a) dos Santos, M. C.; Alvarez, F. *Phys. Rev. B* **1998**, *58*, 13918. (b) Terrones, M.; Redlich, P.; Grobert, N.; Trasobares, S.; Hsu, W. K.; Terrones, H.; Zhu, Y. Q.; Hare, J. P.; Reeves, C. L.; Cheetham, A. K.; Rühle, M.; Kroto, H. W.; Walton, D. R. M. *Adv. Mater.* **1999**, *11*, 655. (c) Terrones, M.; Ajayan, P. M.; Banhart, F.; Blase, X.; Carroll, D. L.; Charlier, J. C.; Crzerw, R.; Foley, B.; Grobert, N.; Kamalakaran, R.; Kohler-Redlich, P.; Rühle, M.; Seeger, T.; Terrones, H. *Appl. Phys. A* **2002**, *74*, 355. (d) Kudashov, A. G.; Okotrub, A. V.; Bulusheva, L. G.; Asanov, I. P.; Shubin, Y. V.; Yudanov, N. F.; Yudanov, L. I.; Danilovich, V. S.; Abrosimov, O. G. *J. Phys. Chem. B* **2004**, *108*, 9048. (e) Lee, Y. T.; Kim, N. S.; Bae, S. Y.; Park, J.; Yu, S. C.; Ryu, H.; Lee, H. J. *J. Phys. Chem. B* **2003**, *107*, 12958.
- (4) Suenaga, K.; Johansson, M. P.; Hellgren, N.; Broitman, E.; Wallenberg, L. R.; Colliex, C.; Sundgren, J. E.; Hultman, L. *Chem. Phys. Lett.* **1999**, *300*, 695.
- (5) (a) Terrones, M.; Terrones, H.; Grobert, N.; Hsu, W. K.; Zhu, Y. Q.; Hare, J. P.; Kroto, H. W.; Walton, D. R. M.; Kohler-Redlich, Ph.; Rühle, M.; Zhang, J. P.; Cheetham, A. K. *Appl. Phys. Lett.* **1999**, *75*, 3932. (b) Terrones, M.; Grobert, N.; Olivares, J.; Zhang, J. P.; Terrones, H.; Kordatos, K.; Hsu, W. K.; Hare, J. P.; Townsend, P. D.; Prassides, K.; Cheetham, A. K.; Kroto, H. W.; Walton, D. R. M. *Nature* **1997**, *388*, 52. (c) Wang, X. B.; Liu, Y. Q.; Zhu, D. B.; Zhang, L.; Ma, H. Z.; Yao, N.; Zhang, B. L. *J. Phys. Chem. B* **2002**, *106*, 2186. (d) Choi, H. C.; Bae, S. Y.; Jang, W. S.; Park, J.; Song, H. J.; Shin, H. J.; Jung, H.; Ahn, J. P. *J. Phys. Chem. B* **2005**, *109*, 1683. (e) Liang, E. J.; Ding, P.; Zhang, H. R.; Guo, X. Y.; Du, Z. L. *Diamond Relat. Mater.* **2004**, *13*, 69. (f) Tang, C.; Bando, Y.; Golberg, D.; Xu, F. *Carbon* **2004**, *42*, 2625.
- (6) (a) Yang, C. M.; El-Merraoui, M.; Seki, H.; Kaneko, K. *Langmuir* **2001**, *17*, 675. (b) Sen, R.; Satishkumar, B. C.; Govindaraj, A.; Harikumar, K. R.; Renganathan, M. K.; Rao, C. N. R. *J. Mater. Chem.* **1997**, *7*, 2335. (c) Nath, M.; Satishkumar, B. C.; Govindaraj, A.; Vinod, C. P.; Rao, C. N. R. *Chem. Phys. Lett.* **2000**, *322*, 333. (d) Sen, R.; Satishkumar, B. C.; Govindaraj, A.; Harikumar, K. R.; Raina, G.; Zhang, J. P.; Cheetham, A. K.; Rao, C. N. R. *Chem. Phys. Lett.* **1998**, *287*, 671. (e) Liu, J. W.; Webster, S.; Carroll, D. L. *J. Phys. Chem. B* **2005**, *109*, 15769.
- (7) (a) Ma, X. C.; Wang, E. G.; Zhou, W. Z.; Jefferson, D. A.; Chen, J.; Deng, S. Z.; Xu, N. S.; Yuan, J. *Appl. Phys. Lett.* **1999**, *75*, 3105. (b) Ma, X. C.; Wang, E. G. *Appl. Phys. Lett.* **2001**, *78*, 978. (c) Lee, C. J.; Lyu, S. C.; Kim, H. W.; Lee, J. H.; Cho, K. I. *Chem. Phys. Lett.* **2002**, *359*, 115. (d) Zhang, G. Y.; Ma, X. C.; Zhong, D. Y.; Wang, E. G. *J. Appl. Phys.* **2002**, *91*, 9324. (e) Yang, J. H.; Kim, B. J.; Kim, Y. H.; Lee, Y. J.; Ha, B. H.; Shin, Y. S.; Park, S. Y.; Kim, H. S.; Park, C. Y.; Yang, C. W.; Yoo, J. B.; Kwon, M.; Ihm, H. K.; Song, H. J.; Kang, T. H.; Shin, H. J.; Park, Y. J.; Kim, J. M. *J. Vac. Sci. Technol. B* **2005**, *23*, 930. (f) Kim, T. Y.; Lee, K. R.; Eun, K. Y.; Oh, K. H.; *Chem. Phys. Lett.* **2003**, *372*, 603.
- (8) Shimoyama, I.; Wu, G.; Sekiguchi, T.; Baba, Y. *J. Electron Spectrosc. Relat. Phenom.* **2001**, *114–116*, 841.
- (9) (a) Wagner, R. S.; Ellis, W. C. *Appl. Phys. Lett.* **1964**, *4*, 84. (b) Morales, A. M.; Lieber, C. M. *Science* **1998**, *279*, 208. (c) Wu, Y. Y.; Yang, P. D. *J. Am. Chem. Soc.* **2001**, *123*, 3165. (d) Stach, E. A.; Pauzauskie, P. J.; Kuykendall, T.; Goldberger, J.; He, R. R.; Yang, P. D. *Nano Lett.* **2003**, *3*, 867. (e) *Chemistry and Physics of Carbon*; Baker, R. T. L., Barber, M. A., Walker, P. L., Thrower, P. A., Eds.; Dekker: New York, 1978; Vol. 14, p 83. (f) Gavillet, J.; Loiseau, A.; Journet, C.; Willaime, F.; Ducastelle, F.; Charlier, J. C. *Phys. Rev. Lett.* **2001**, *87*, 275504.
- (10) (a) Tian, Y. J.; Hu, Z.; Yang, Y.; Wang, X.; Chen, X.; Xu, H.; Wu, Q. *J. Am. Chem. Soc.* **2004**, *126*, 1180. (b) Yang, Y.; Hu, Z.; Tian, Y. J.; Lü, Y. N.; Wang, X. Z.; Chen, Y. *Nanotechnology* **2003**, *14*, 733. (c) Wang, X. Z.; Hu, Z.; Wu, Q.; Chen, Y. *Chin. Phys. Lett.* **2001**, *10*, 76.
- (11) (a) Hurd, C. D.; Simon, J. I. *J. Am. Chem. Soc.* **1962**, *84*, 4519. (b) Hore, N. R.; Russel, D. K. *J. Chem. Soc., Perkin Trans. 2* **1998**, *2*, 269. (c) Ikeda, E.; Mackie, J. C. *J. Anal. App. Pyrolysis* **1995**, *34*, 47. (d) Tan, H. Z.; Liao, X. W.; Xu, T. M.; Zhao, K.; Hui, S. E.; Che, D. F. *Journal of Xi'an Jiao Tong University* **2004**, *38*, 251.
- (12) (a) Casanovas, J.; Ricart, J. M.; Rubio, J.; Illas, F.; Jimenez-Mateos, J. M. *J. Am. Chem. Soc.* **1996**, *118*, 8071. (b) Souto, S.; Pickholz, M.; dos Santos, M. C.; Alvarez, F. *Phys. Rev. B* **1998**, *57*, 2536.
- (13) (a) Hofmann, S.; Csányi, G.; Ferrari, A. C.; Payne, M. C.; Robertson, J. *Phys. Rev. Lett.* **2005**, *95*, 36101. (b) Hofmann, S.; Ducati, C.; Robertson, J.; Kleinsorge, B. *Appl. Phys. Lett.* **2003**, *83*, 135. (c) Helveg, S.; Lopez-Cartes, C.; Sehested, J.; Hansen, P. L.; Clausen, B. S.; Rostrup-Nielsen, J. R.; Abild-Pedersen, F.; Nørskov, J. K. *Nature* **2004**, *427*, 426.
- (14) (a) Diamond, S.; Trans, C. W. *AIIME* **1967**, *239*, 705. (b) Mojica, J. F.; Levenson, L. L. *Surf. Sci.* **1976**, *59*, 447.
- (15) Cussler, E. L. *Diffusion — Mass transfer in fluid systems*, 2nd ed.; Translated by Wang, Y. X., Jiang, Z. Y., Chen, Z. L., Xin, T., Eds.; Chemical Industry Press: Beijing, 2000.